Electronic Supplementary Information

Sub-nanometric synthesis of Cu_2O catalyst for Pd-free C-C coupling reactions

Ankit Agrawal,[a,b‡] Reena Goyal,[c,e‡] B. Moses Abraham,[d] Omvir Singh, ,[a,b] Mukesh K Poddar,[e] Shailendra Tripathi,[a] Rajaram Bal,*[e] and Bipul Sarkar,*[a,b]

[a] Catalytic De-Polymerization Area, Upstream & Wax Rheology Division, CSIR-Indian Institute of Petroleum, Dehradun 248005, India
E-mail: bsarkar@iip.res.in
[b] Academy of Scientific and Innovative Research (AcSIR), CSIR-HRDC Campus, Sector 19, Kamla Nehru Nagar, Ghaziabad, Uttar Pradesh 201002, India
[c] Department of Chemical Engineering, Indian Institute of Technology-Roorkee, Roorkee-247667, Uttarakhand, India
[d] Advanced Centre of Research in High Energy Materials (ACRHEM), University of Hyderabad, Prof. C. R. Rao Road, Gachibowli, Telangana, Hyderabad 500046, India
[e] Nano Catalysis Area, Catalytic Conversion and Process Division, CSIR-Indian Institute of Petroleum, Dehradun 248005, India
E-mail: raja@iip.res.in
‡ Both authors contribute equally.

Figure S1

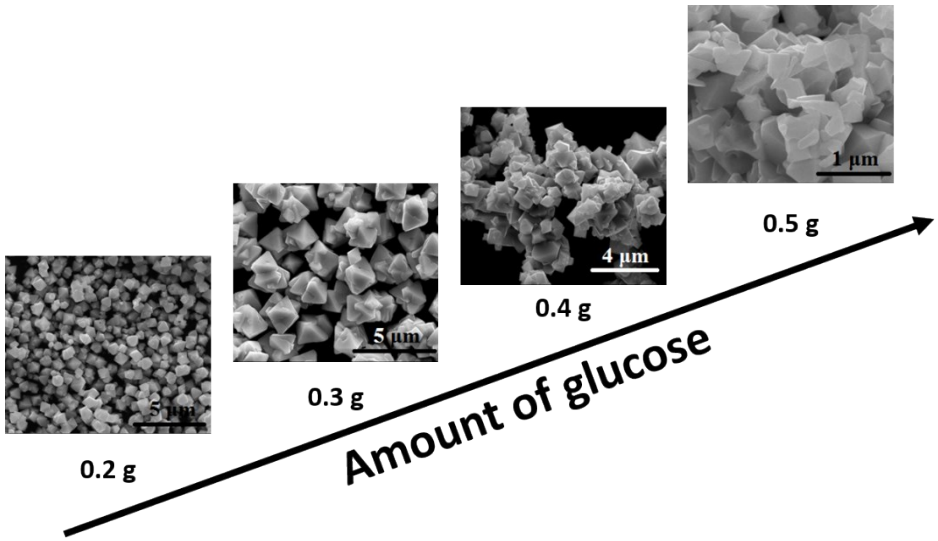

Figure S1. Effect of glucose on the shape-selective synthesis of Cu_2O nanostructures.

Figure S2

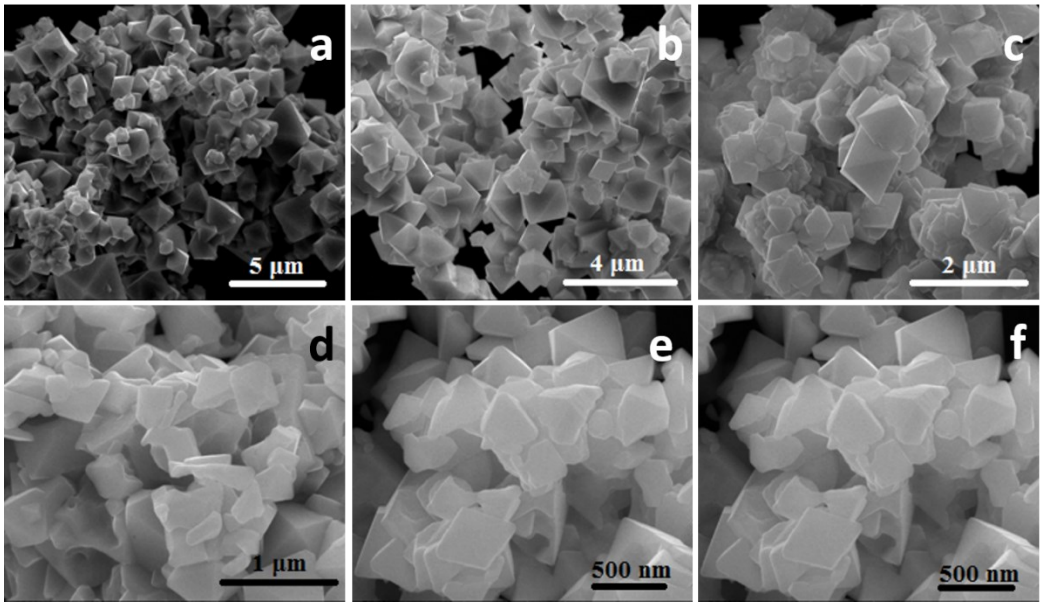

Figure S2. SEM micrographs of Cu_2O nanocrystals: (a-c) synthesised in the absence of NaOH solution and (d-f) with 5, 10 and 20 nmol NaOH solution.

Figure S3.

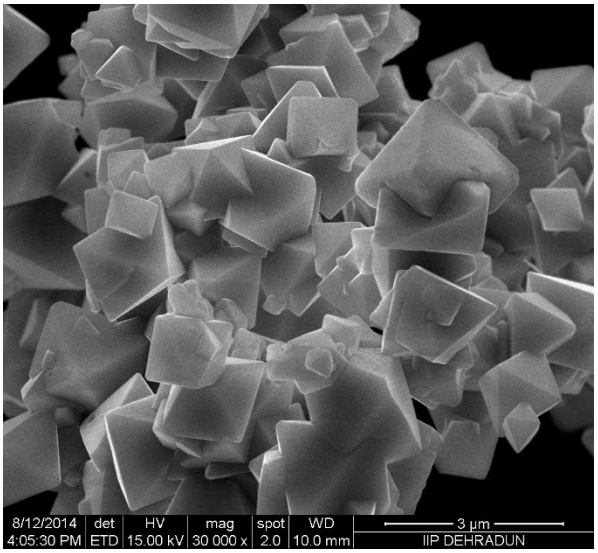

Figure S3. Morphology obtained during high temperature (90°C) sonicated sample.

Figure S4.

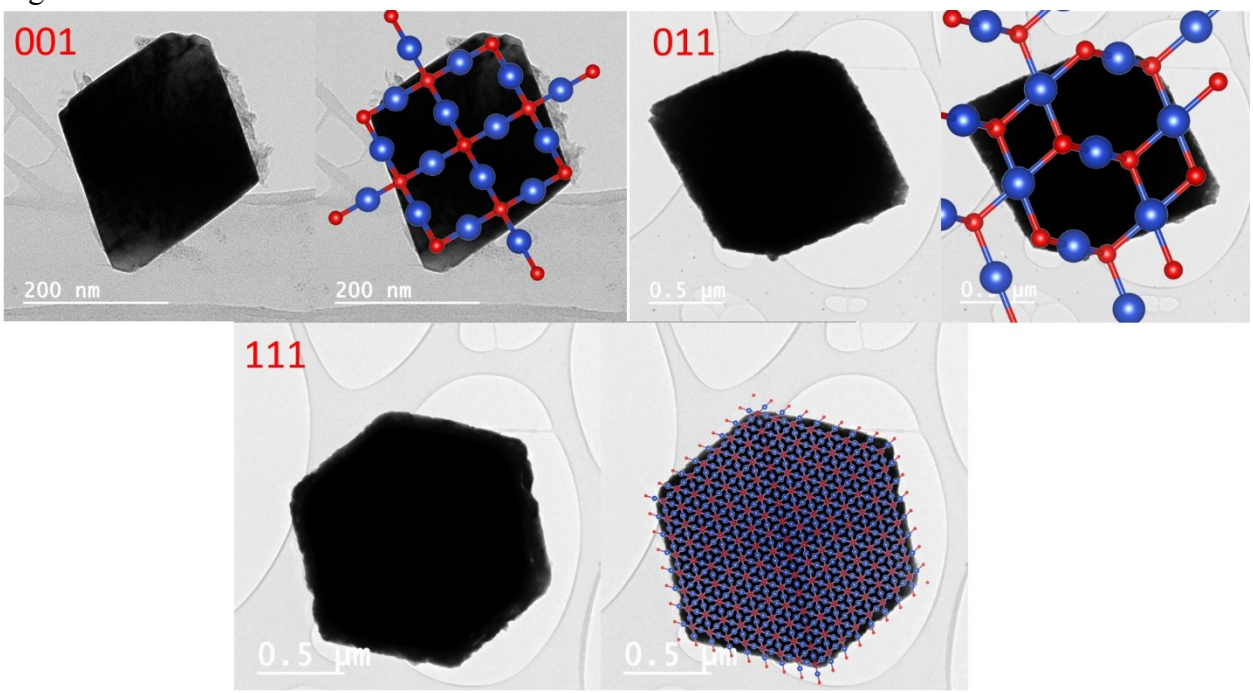

Figure S4. TEM images of the well-defined Cu_2O facets.

Figure S5.

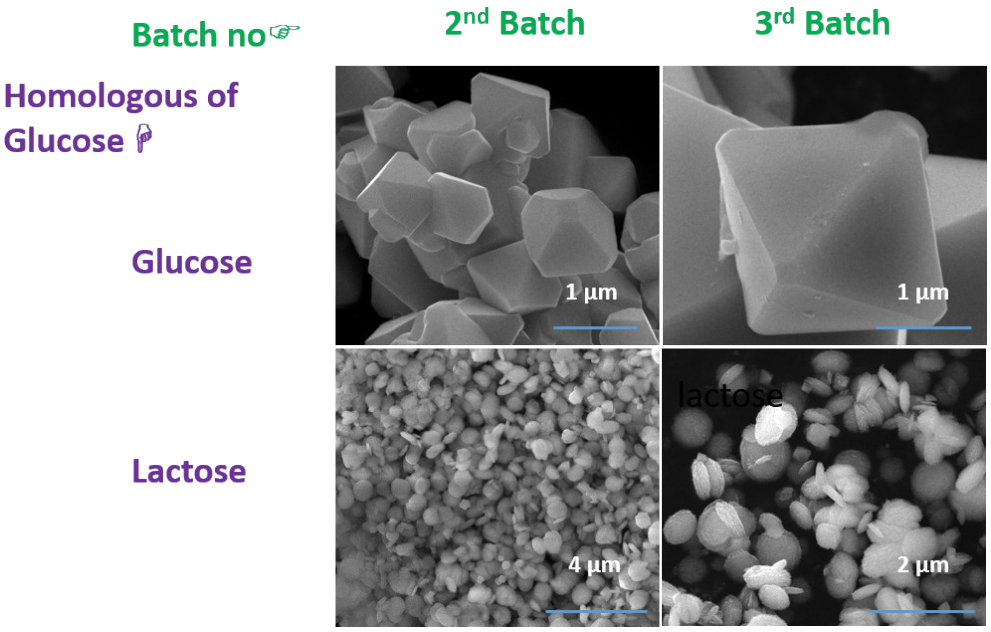

Figure S5. SEM micrographs of Cu_2O nano crystals: Effect on the morphology after the regeneration of catalyst.

Figure S6

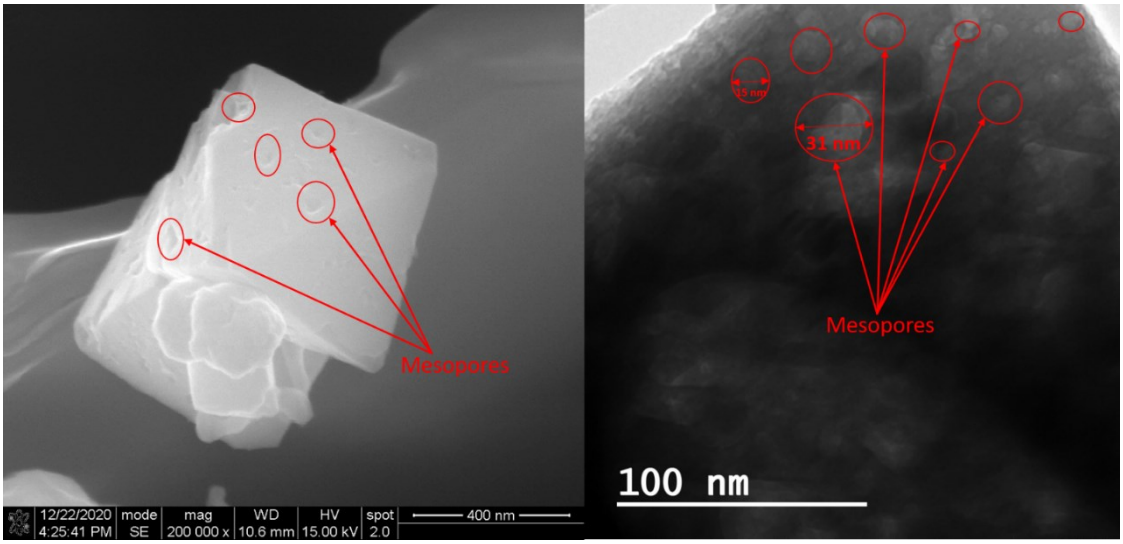

Figure S6. SEM and TEM images of Cu_2O mesopores.

Figure S7

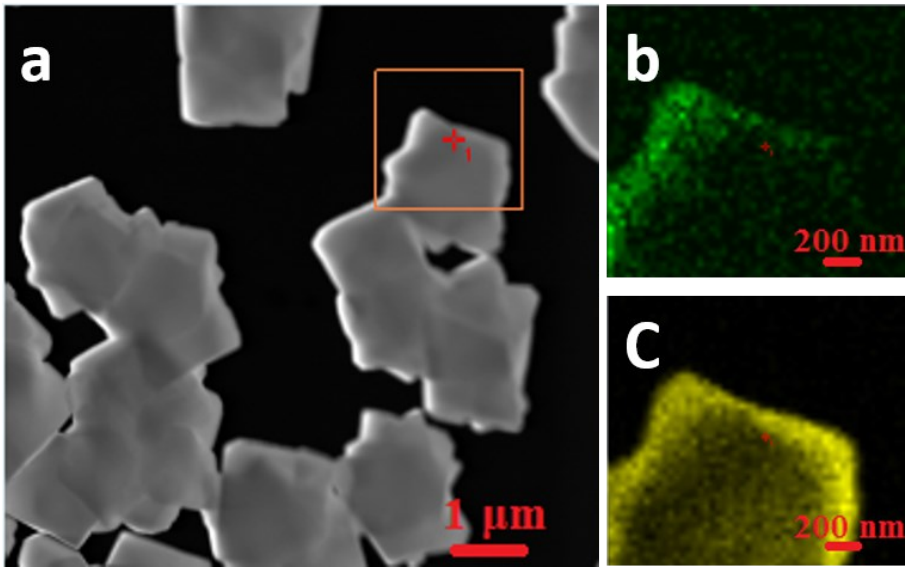

Figure S7. Elemental mapping of Cu and O of the corresponding TEM image.

Figure S8.

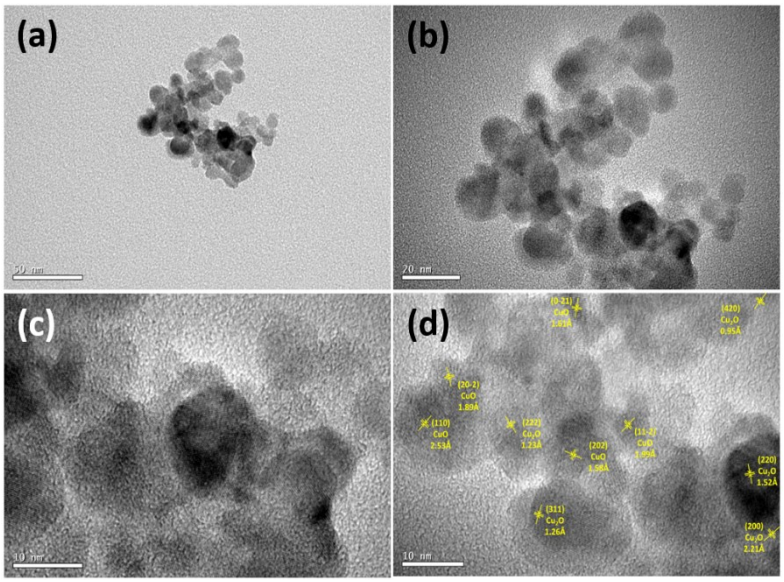

Figure S8. TEM images of the spent Cu_2O nanocrystals.

Figure S9

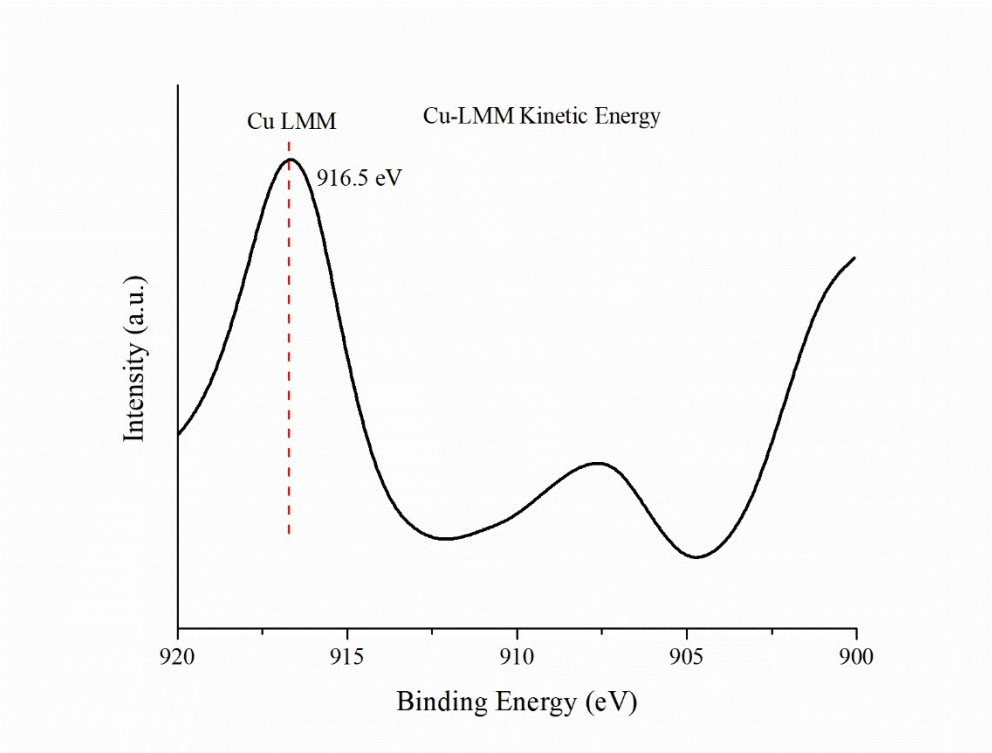

Figure S9. XAES (Cu-LMM) spetcrum of Cu_2O nanocrystals.

Figure S10

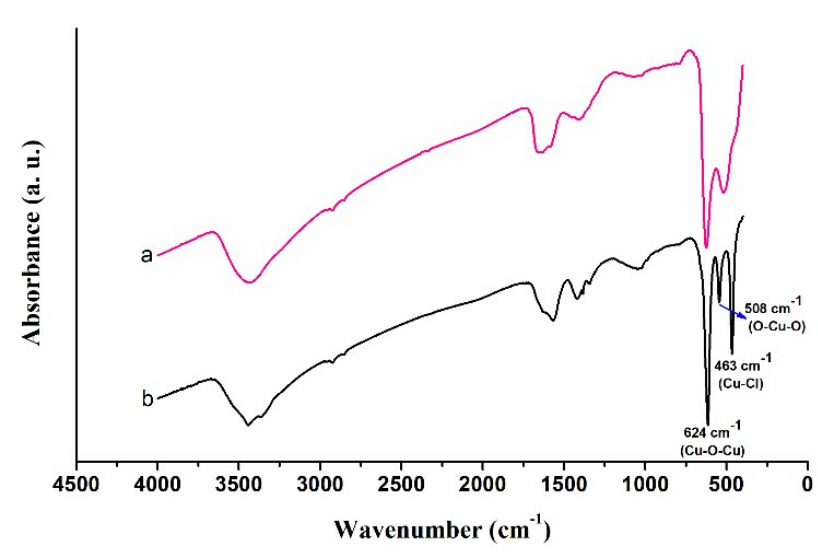

Figure S10. FT-IR spectra of Cu_2O nanocrystals (a) octahedral and (b) collected during the reaction with Cl-benzene.

Figure S11.

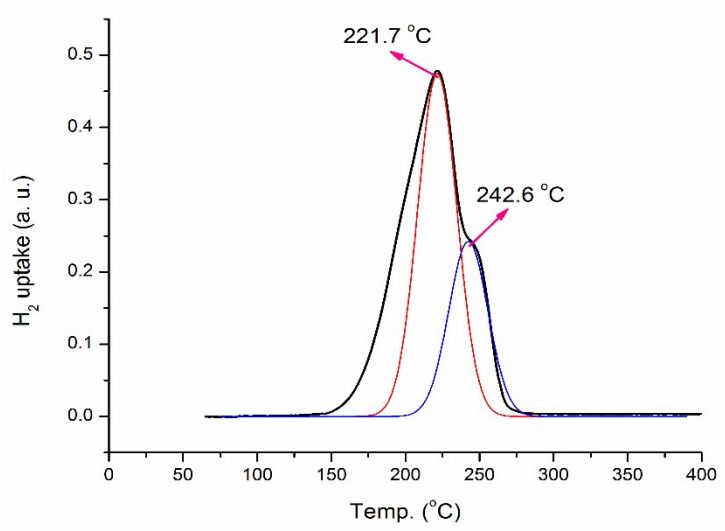

Figure S11. TPR pattern of the Cu_2O mesocage prepared via pulse mode sonication of copper(II) acetate.

Figure S12

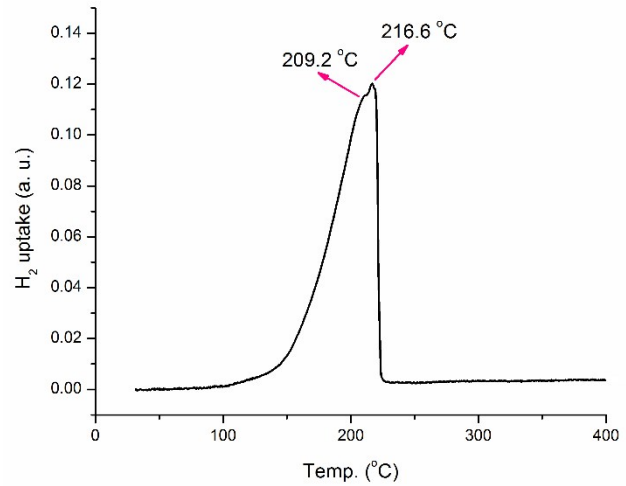

Figure S12. TPR of porous Cu_2O prepared via pulse mode sonication of copper(II) acetate.

Figure S13

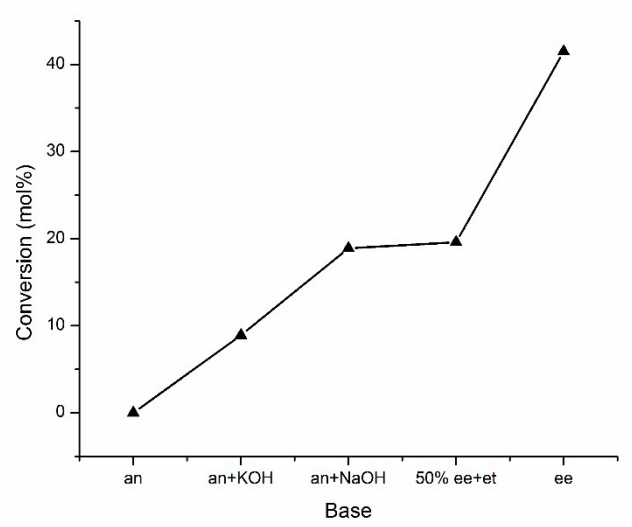

Figure S13. Effect of solvent polarity on the homocoupling of Iodobenzene. (where an= acetonitrile, ee=2-(Ethylamino)ethanol)

Figure S14

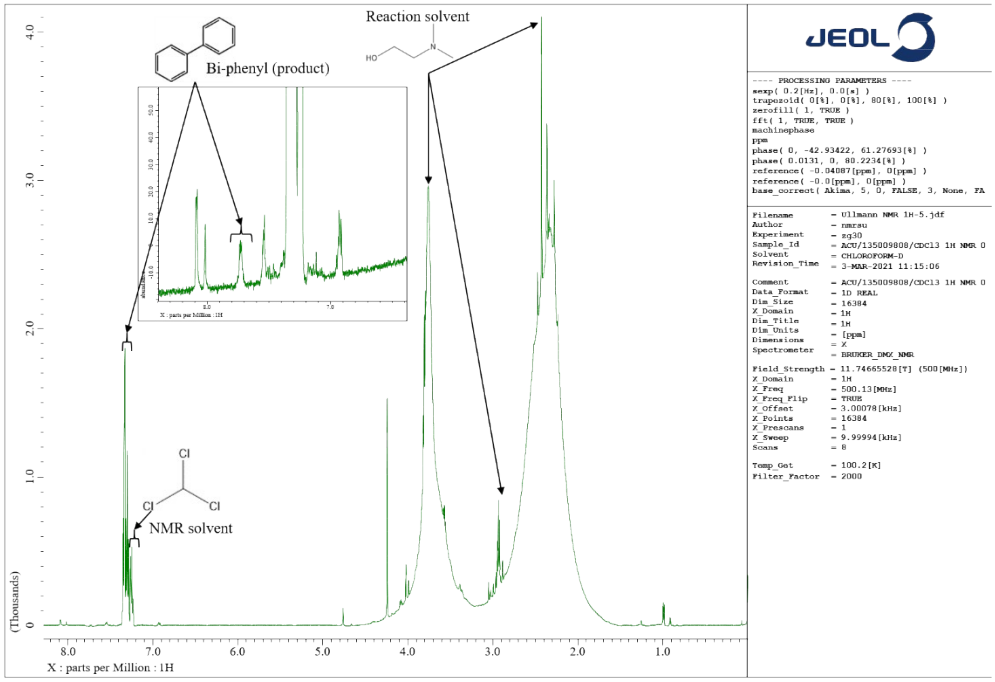

Figure S14. ^{1}H NMR of the representative products obtained from the homocoupling of chlorobenzene.

Figure S15

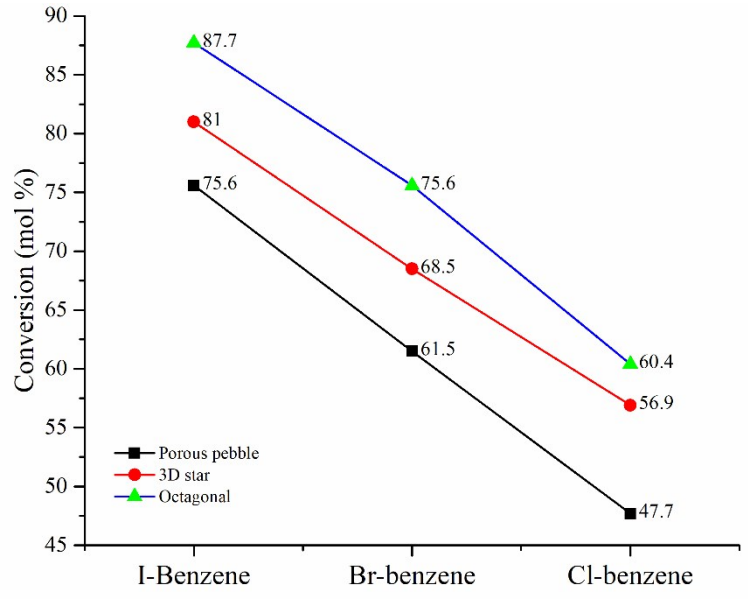

Figure S15. Effect of morphology on the conversion of Ar-X (X= Cl, Br, I)